Archives of Dermatological Research (2019) 311:741–751
https://doi.org/10.1007/s00403-019-01962-5

ORIGINAL PAPER

Substrate softness promotes terminal differentiation of human keratinocytes without altering their ability to proliferate back into a rigid environment

Choua Ya[1,2] · Mariana Carrancá[1] · Dominique Sigaudo-Roussel[1] · Philippe Faure[3] · Bérengère Fromy[1] · Romain Debret[1]

Received: 29 October 2018 / Revised: 13 May 2019 / Accepted: 15 June 2019 / Published online: 7 August 2019

Abstract

Substrate stiffness is a key regulator of cell behavior. To investigate how mechanical properties of cell microenvironment affect the human keratinocyte, primary cells were seeded on polyacrylamide hydrogels of different compliances (soft: 4 kPa, medium: 14 kPa, rigid: 45 kPa) in comparison with glass coverslip (> GPa). Keratinocyte spreading and proliferation were strongly decreased on the softest hydrogel, while no significant difference was observed between medium, rigid hydrogels and glass coverslip, and cells' viability was comparable in all conditions after 72 h. We then performed a RNA-seq to compare the transcriptomes from keratinocytes cultured for 72 h on the softest hydrogel or on coverslips. The cells on the soft hydrogel showed a strong increase in the expression of late differentiation marker genes from the epidermal differentiation complex (1q21) and the antioxidant machinery. In parallel, these cells displayed a significant loss of expression of the matrix receptors (integrin α6 and β1) and the EGF receptor. However, when these cells were replated on a plastic culture plate (> GPa), they were able to re-engage the proliferation machinery with a strong colony-formation efficiency. Overall, using low-calcium differentiation monolayers at confluence, the lesser the rigidity, the stronger the markers of late differentiation are expressed, while the inverse is observed regarding the markers of early differentiation. In conclusion, below a certain rigidity, human keratinocytes undergo genome reprogramming indicating terminal differentiation that can switch back to proliferation in contact with a stiffer environment.

Keywords Mechanical properties · Keratinocytes · Differentiation · Proliferation · Transcriptome profiling

Introduction

In the epidermis, the balance between keratinocyte proliferation in the basal layer and terminal differentiation and shedding in the upper layers maintain normal tissue homeostasis [3]. The keratinocytes are interconnected via intercellular junctions and lie on a basal membrane at the interface of the epidermis and the dermis, the underlying extracellular matrix (ECM)-rich connective tissue. Mechanical, biophysical and biochemical factors regulate the keratinocyte function. Indeed, physical interactions are detected by the keratinocytes through mechanotransduction mechanisms transforming mechanical loads into biochemical cascades and have been involved in the regulation of keratinocyte proliferation, differentiation, morphology, and migration [27]. There has been extensive research into the measurement of the skin's elastic modulus via a multitude of in vitro and in vivo techniques with various values depending on

Bérengère Fromy and Romain Debret are co-last authors.

Electronic supplementary material The online version of this article (https://doi.org/10.1007/s00403-019-01962-5) contains supplementary material, which is available to authorized users.

✉ Romain Debret
romain.debret@ibcp.fr

[1] CNRS/UCBL, University Lyon 1, UMR 5305, Laboratory of Tissue Biology and Therapeutic Engineering, LBTI, IBCP, 7, passage du Vercors, 69367 Lyon cedex 7, France

[2] Isispharma, 29 Rue Maurice Flandin, 69003 Lyon, France

[3] Alpol Cosmétique, 140 Rue Pasteur, 01500 Château-Gaillard, France

the method used (see [6, 11] for comprehensive reviews). In vivo, the mechanical measurements obtained are generally attributed to those of the dermis because of its thickness with respect to the epidermis, with a rigidity of 5 and 10 kPa as measured by indentation [30]. The dermis is a connective tissue composed mainly of fibroblasts responsible for the synthesis of an ECM rich in collagen fibers, elastic fibers, glycosaminoglycans and the fundamental substance. Mechanically speaking, the dermis gives the skin its strength, firmness, elasticity and viscosity. Studies have attempted to measure the mechanical properties of the different histological layers of the skin, but high interconnections between the different layers rendered the discrimination challenging.

The mechanical properties of the skin can be altered by physiological phenomena such as aging or wounding [9, 30], or by pathological phenomena with consequences on the epidermal homeostasis [10]. During chronological aging, the expression level of ECM constituents, such as type I and III collagens [23] and elastin [7], decrease, while the synthesis and the activities of matrix metalloproteases increase [24]. Together, these alterations lead to age-related reduction of skin elastic modulus as reported in humans [30]. During the wound healing process, the composition and structure of the ECM are continuously modified during the formation of granulation tissue and remodeling [8], inducing drastic changes in the mechanical properties of the dermis. Indeed, the rigidity of the granulation tissue increased from 18 kPa at 7 days after wounding to 50 kPa at 12 days [9]. This increase is required for the initiation of keratinocyte migration. Persistent abnormal alterations in the mechanical properties of ECM would therefore contribute to healing defects such as chronic or hypertrophic wounds [12].

In vitro studies showed that keratinocytes are able to respond to the rigidity of the support. Studies on the HaCaT cell line have indeed shown that the rigidity of the support promotes proliferation and migration, leading to an increase in re-epithelization, whereas cell differentiation is inhibited [25]. The substrate stiffening promotes proliferation by activation of the EGF signaling pathway, as reported using primary human keratinocytes [13]. In addition, the rigidity of the substrate regulated the formation of adhesion junctions via activation of the Jun N-terminal kinase pathway [29]. Finally, stiffness affects the morphology of cells resulting in a decrease in cell spread and focal adhesions [22]. The changes in the dermal stiffness could thus explain the phenotypic disturbances observed in keratinocytes leading to an alteration of epidermal homeostasis.

However, data on the impact of skin stiffness on epidermal differentiation are still very sparse, particularly using primary human cells. In this study, we aimed to investigate how mechanical properties of the microenvironment affect primary human keratinocyte phenotype. For this purpose, we used primary human keratinocytes grown on substrates of different compliances.

Materials and methods

Ethical considerations

Infant foreskins were collected according to the Declaration of Helsinki Principles. Written informed consent was obtained from infants' parents according to French bioethical law of 2004.

Cell culture

The human epidermal keratinocyte cultures were obtained from child foreskin biopsies after enzymatic treatment [1]. Briefly, the biopsies were cut into small pieces and immersed overnight at 4 °C in a solution containing trypsin (Gibco, Life Technologies, Carlsbad, CA, USA) and dispase (Dispase II; Roche Diagnostics, Mannheim, Germany). Then, the dermis and epidermis were separated and the epidermis was incubated for 20 min at 37 °C with trypsin and 0.05% EDTA. The cells were resuspended and filtered through a 70 µm cell stainer (BD Biosciences) to remove the remaining aggregates. After extraction, keratinocytes were cultured in KGM2 medium (Keratinocyte Growth Medium 2, Promocell, Heidelberg, Germany) comprising 0.06 mM $CaCl_2$ and supplemented with 100 µg/ml of primocin at 37 °C and 5% CO_2. Cells were amplified on plastic dishes prior to seeding on different substrates for experimental assessments. To induce keratinocyte differentiation, at confluence, cells were cultured in KGM2 without growth factor supplement. The cells were used at early passage (passage 1 and 2) in subsequent experiments. All cell-based in vitro experiments were repeated in triplicate.

Generation of polyacrylamide hydrogels

The hydrogels were synthesized according to the principle described previously by Tse and Engler [2]. Briefly, 18 mm diameter coverslips were activated with 70 mM NaOH solution and heated at 80 °C. This step was repeated with milliQ water until NaOH forms a thin semi-transparent film. The coverslips were treated for 5 min with APES (3-aminopropyltriethoxysilane, Sigma) and thoroughly rinsed. Then, 0.5% glutaraldehyde (Sigma) was added onto the coverslips for 30 min and dried few minutes at room temperature. In parallel, 24 × 60 mm glass slides were chlorosilanized with DCDMS (dichlorodimethylsilane, Sigma) for 5 min, gently rinsed, and dried for 30 min at room temperature.

Polyacrylamide gels with different modulus of elasticity values were produced by mixing acrylamide/bis-acrylamide

solutions at final percentages (p/v) of 3/0.1, 4/0.225 and 10/0.225 for soft, medium and rigid hydrogels, respectively. The polymerization is initiated with APS (ammonium persulfate, Sigma) and TEMED (*N*,*N*,*N*′,*N*′-tetramethylethane-1,2-diamine, Sigma). The polyacrylamide solution is immediately pipetted onto the chlorosilanized slide and covered by the functionalized coverslip. After the completed polymerization, the top coverslip with the attached polyacrylamide gel is slowly peeled off and rinsed to take out DCDMS on gel surface.

To facilitate keratinocyte attachment, a heterobifunctional crosslinker, sulfo-SANPAH (sulfosuccinimidyl6(4-azido-2-nitrophenyl-amino)hexanoate, ThermoFisher Scientific), is used to crosslink extracellular matrix molecules onto the surface of the gel. 0.2 mg/mL sulfo-SANPAH solution is added to the gel surface, placed 3 inches under an ultraviolet lamp, irradiated for 10 min and rinsed with water. Then, 100 µg/mL of rat tail collagen I solution (ThermoFisher Scientific) is added to the gel and incubated for 2 h at room temperature under a 50 rpm agitation. Hydrogels were rinsed in PBS (phosphate buffered saline), placed in 12-well plates and immersed in culture media at 37 °C one night prior to cell seeding.

Mechanical characterization of polyacrylamide hydrogels

Viscoelastic properties of polyacrylamide gels (12 mm diameter and ~ 1.2 mm thick) were determined by Dynamical Mechanic Analysis (DMA 242 E Artemis, NEZSTCH, Germany). Samples were subject to compression tests under liquid immersion (PBS) water bath at room temperature. Strain-sweep measurements were performed to determine the elastic limit or linear domain of the gels. The tan delta, complex modulus (E^*) as well as storage (E') and loss modulus (E'') were determined from dynamic stress curves obtained for an amplitude of 55 µm, a frequency of 1 Hz and 10% constraint.

Immunofluorescence

Keratinocytes were plated on a glass coverslip or polyacrylamide gels in 12-well plates for 24 h to analyze cell morphology, or for 72 h to observe differentiation markers. Then, the cells were fixed in 4% paraformaldehyde for 10 min.

To visualize focal adhesion and actin cytoskeleton, cells were permeabilized with 0.1% Triton X-100 for 10 min, blocked with 5% of goat serum in PBS for 1 h at room temperature and incubated with anti- antibody (clone 8D4, Sigma) overnight at 4 °C. Secondary Alexa-488 anti-mouse (Invitrogen) was incubated 1 h at room temperature. Actin network was stained with TRITC phalloidin for 5 min at room temperature. Differentiation markers were immuno-detected with anti-K10 (Ab76318, Abcam, 1:500) or anti-involucrin (Ab53112, Abcam, 1:500) for 2 h at room temperature. Secondary Alexa-563 anti-rabbit (Invitrogen) was incubated for 1 h at room temperature.

All stainings were incubated with DAPI (4,6-diamidino-2-phenylindole) to visualize DNA and mounted with Permafluor™ Aqueous Mounting Medium (Labvision, Thermo Fisher Scientific). All images were acquired with a Nikon TiE inverted fluorescent microscope.

Cell proliferation and viability assay

Cells (5×10^3 per substrate) were seeded on glass coverslip or polyacrylamide hydrogels. Cells were fixed at 24 h, 48 h and 72 h with 4% paraformaldehyde for 10 min and stained with DAPI for 5 min. Cell proliferation was determined by nuclei count using ImageJ software. All experiments were repeated at least three times in triplicate.

To assess keratinocyte viability, cells were cultured on glass coverslip or on hydrogels for 3 days. Cells were then stained with LIVE/DEAD™ Cell Imaging Kit (Invitrogen), as described by the manufacturer's protocol. Green living cells and red dead cells were counted and the ratio of living cells/dead cells was expressed as a percentage of cell viability.

mRNA extraction and qRT-PCR

Total RNA was extracted from cells at indicated times using RNeasy mini kit (Qiagen, Valencia, CA) according to the manufacturer's instructions. Reverse transcription was performed using PrimeScript™ RT Reagent Kit (Takara, Tokyo, Japan). qRT–PCR was performed on a Mx3000P real-time PCR system (Stratagene, san Diego, CA, USA) using SYBR® Premix Ex Taq™ II (TaKaRa). Amplification was started at 95 °C for 30 s as the first step, followed by 40 successive cycles of PCR: at 95 °C for 5 s, at 60 °C for 30 s and at 72 °C for 30 s. Primers specific for RPL13 (ribosomal housekeeping gene), MKI67 (proliferation marker), KRT1 and KRT10 (early differentiation marker), IVL, TGM1, FLG and CDSN (late differentiation markers), ITGA6 and ITGB1 (cell adhesion), CDKN1A and CDKN2A (cell cycle progression), EREG and EGFR (epidermal growth factor signaling), MT1H, AKR1B10 and AKR1C2 (oxidative machinery) were used.

Western blot

To analyze protein expression, cells were washed briefly in PBS and lysed on ice in the RIPA buffer (50 mM Tris–HCl, pH 8, 150 mM NaCl, 1% Nonidet P-40, 0.1% sodium deoxycholate, 0.1% SDS, 1 mM orthovanadate and protease inhibitor cocktail (Thermo Fischer scientific). Lysates were

centrifuged for 10 min at 14,000*g* at 4 °C to eliminate cell debris. Proteins were separate by SDS–PAGE followed by transfer to polyvinylidene fluoride membrane (EMD-Millipore, Billerica, MA). The membrane was blocked with 5% non-fat milk in Tris-buffered saline (TBS) buffer containing 0.1% Tween-20, and incubated with rabbit anti-involucrin (SY5) antibody (SC-21,748, Santa Cruz, 1:1000) and mouse anti-actin (C4, MAB1501, Sigma-Aldrich, 1:5000), overnight at 4 °C. The membrane was incubated with secondary antibodies for 1 h at room temperature: goat anti-rabbit IgG (H + L)–HRP conjugate (170–6510, Biorad, 1:10,000) and goat anti-mouse IgG (H + L)–HRP conjugate (170–6516, Biorad, 1:10,000). Antibody binding was detected by the enhanced chemiluminescence system (Thermo Fischer Scientific), using the Fusion Fx system (Vilbert Lourmat).

RNA sequencing

Cells were cultured on glass substrate and soft hydrogel for 3 days and total RNA was extracted using RNeasy mini kit (Qiagen). RNA quantity and purity were verified using 2200 TapeStation system (Agilent Technologies). Library preparation was performed using mRNA-Seq Library Prep Kit Lexogen following manufacturer's instructions. Libraries were validated on TapeStation—HSD1000 ScreenTape®Dosage. Barecoded libraries were pooled together (three per run) on an equimolar basis and run using PI chips on an Ion Torrent™ PGM sequencer using HiQ chemistry. Library preparation and sequencing were achieved by the IGFL sequencing platform (Lyon, France).

Bioinformatic analyses

Reads were aligned to the human reference genome hg19 using the Ion Torrent RNASeqAnalysis plugin. Two consecutive alignments were achieved through the STAR and Bowtie2 programs to generate the BAM files. Reads over genes were determined using the R/Bioconductor "Rsubread" software package to create a count matrix [15]. Differential gene expression analysis was performed using R/Bioconductor "limma" and "edgeR" software packages [18, 20, 21]. Smear plot and heat map were generated from limma-voom normalized values in *R* [14]. Genes with a differential expression FDR ≤ 0.05 were considered significant. Two sets of significant genes, upregulated or downregulated, were subjected to gene ontology (GO) analysis using GOrilla tool [5] and enrichment analysis of the five top molecular functions are represented.

Clonogenic assay

Primary keratinocytes were plated on soft hydrogel or glass coverslip for 3 days then clonogenic assay was realized on three generations with plastic culture plate. For each generation, the cells were trypsinized, resuspended in the media and counted. The cells were re-seeded (500 cells/well) in 6-well plates and incubated for 10 days. On the 10th day, cells were trypsinized, counted and re-seeded (500 cells/well) in new 6-well plates. In parallel, cells were fixed with 4% paraformaldehyde solution for 10 min and the colonies were stained with 0.1% crystal violet for 1 h. The wells were rinsed three times with PBS and cells were lysed with 2% SDS solution. The absorbance (570 nm) was read with Tecan Infinite 1000 M. All experiments were performed in triplicate.

Statistical analysis

All data were presented as mean ± SD for three independent experiments. Statistical significance ($p < 0.05$) was determined by performing either unpaired *T* test when comparing two groups or one-way or two-way analysis of variance (ANOVA) followed by a Bonferroni post-test when comparing multiple groups. All analyses were performed with GraphPad Prism5 software.

Results

To investigate human keratinocyte behavior in response to substrate stiffness, we used polyacrylamide hydrogels (PAH) of different compliances and functionalized with type I collagen coating to allow cell adhesion. The three different PAH preparations displayed E^* of 3.91 ± 1.4 kPa (soft), 14.63 ± 3.7 kPa (medium) and 44.98 ± 3.6 kPa (rigid), respectively (Fig. 1a). 24 h post-seeding, the morphology of freshly isolated human keratinocytes was modified by the substrate stiffness (Fig. 1b). On soft PAH, the cell shape remained round with a thin distribution of the actin cytoskeleton at the plasma membrane, while no clear focal adhesion point was observed. On medium and rigid PAH, cells were much more spread as illustrated by a wider distribution of actin and the presence of well-defined focal adhesion points. Glass coverslip condition was characterized by the formation of stress fibers across the cytoplasm and well-defined focal adhesion points at the cell periphery leading to a polygonal cell shape. Since cells were present in all conditions, their proliferation was assessed by cell counting during 3 days (Fig. 1c). No significant difference was observed between medium PAH, rigid PAH and glass coverslip conditions. In contrast, no proliferation was noted on the soft substrate. Cell viability was then assessed in all conditions after 3 days and no significant difference was observed (Fig. 1d). These results show that the human keratinocyte gradually adapts to the substrate rigidity on which it adheres. On the softest substrate, although the cells were in the proliferative phase

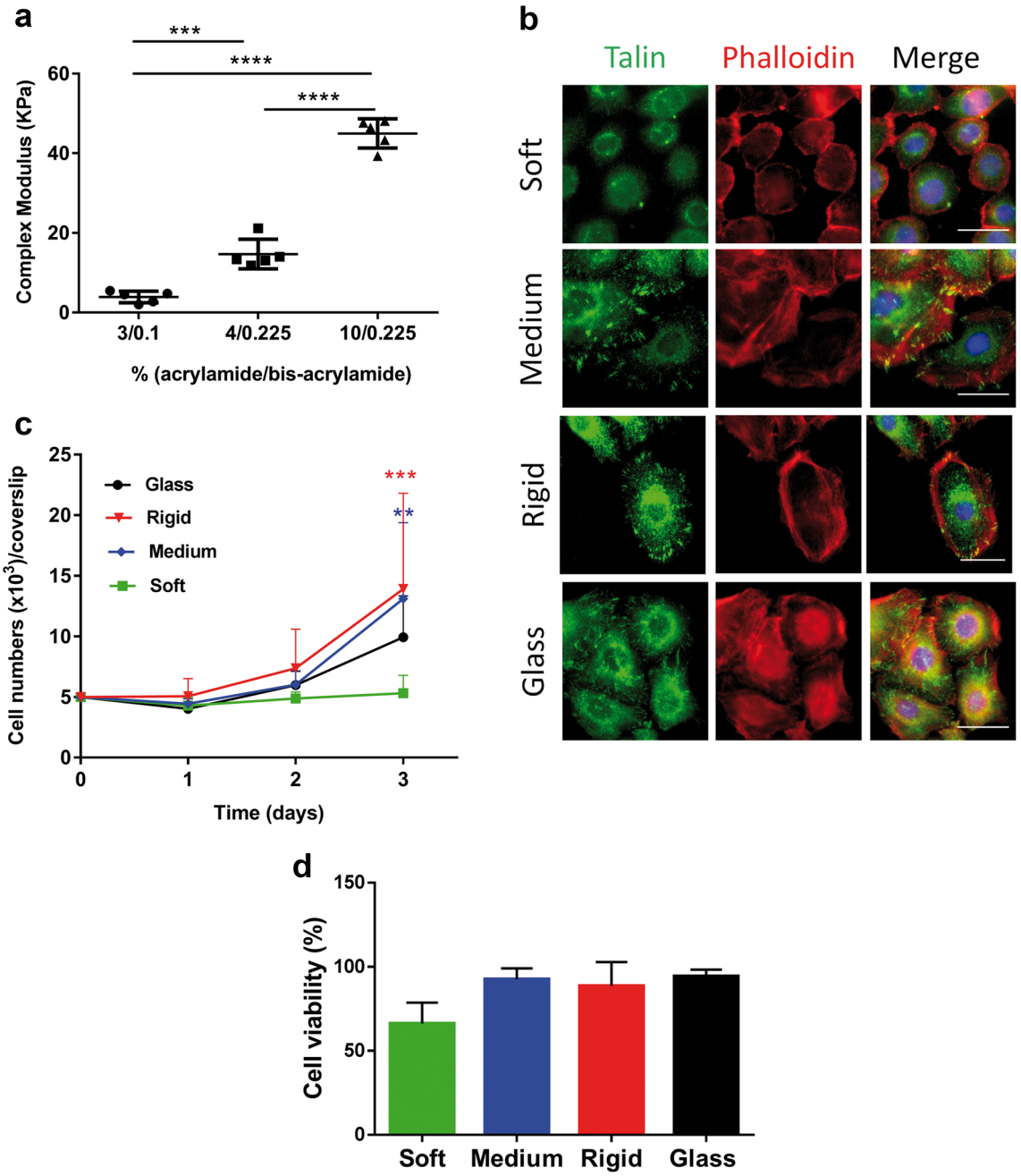

Fig. 1 Substrate mechanical properties affect keratinocyte behavior. **a** Viscoelastic properties of PAH were determined by dynamical mechanic analysis, using an amplitude of 55 µm, a frequency of 1 Hz and 10% constraint. (E^*) complex modulus. ($n=5$) The data are presented as mean ± SD; $^{***}P<0.001$ and $^{****}P<0.0001$ using one-way ANOVA with a Bonferroni post-test. **b** Human primary keratinocytes were cultured on glass and PAH with different rigidities. After 24 h, cells were stained for F-actin content (phalloidin staining: red) and nuclei were counterstained with DAPI (blue). Immunostained for talin (green) after 24 h in culture. Scale bar: 25 µm. **c** Human primary keratinocytes were cultured on glass (black dot), soft (green square), medium (blue diamond) and rigid (red triangle) PAH. Nuclei were counterstained with DAPI and proliferation rate was measured by cell counting after 1, 2 and 3 days in culture. ($n=3$) All data are presented as mean ± SD, $^{**}P<0.01$ and $^{***}P<0.001$, using two-way ANOVA with a Bonferroni post-test, compared to soft PAH condition. **d** After 3 days in culture on PAH with different rigidities or glass coverslip, living cells and dead cells were visualized and counted by LIVE/DEAD™ Cell Imaging. Histograms represent cell viability as the percentage of living cells over dead cells. All data are presented as mean ± SD. A two-way ANOVA with a Bonferroni post-test was applied, compared to soft PAH condition

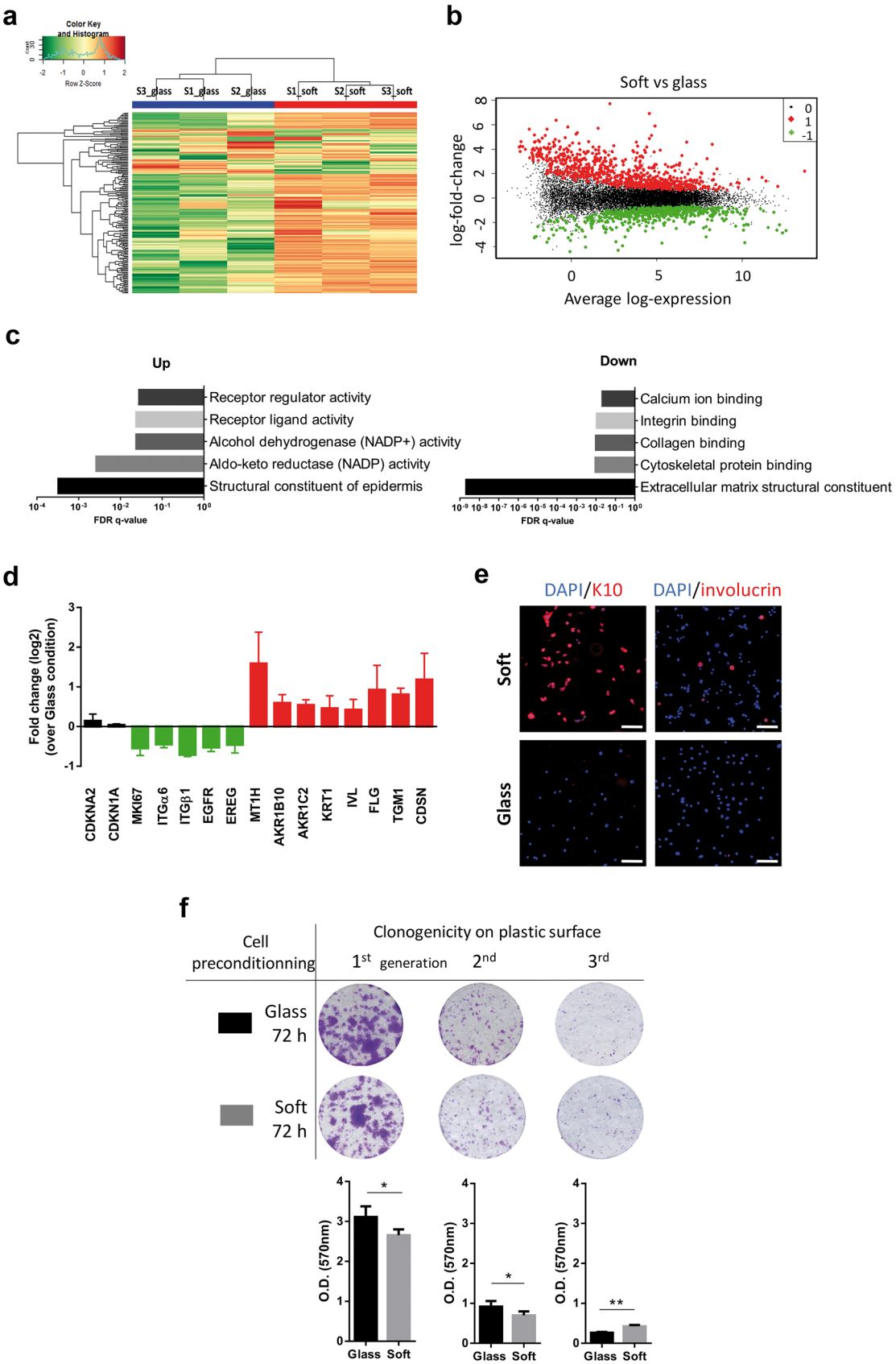
a
Color Key and Histogram
Row Z-Score
S3_glass
S1_glass
S2_glass
S1_soft
S2_soft
S3_soft
b
Soft vs glass
log-fold-change
Average log-expression
c
Up
Receptor regulator activity
Receptor ligand activity
Alcohol dehydrogenase (NADP+) activity
Aldo-keto reductase (NADP) activity
Structural constituent of epidermis
FDR q-value
Down
Calcium ion binding
Integrin binding
Collagen binding
Cytoskeletal protein binding
Extracellular matrix structural constituent
FDR q-value
d
Fold change (log2) (over Glass condition)
CDKNA2
CDKN1A
MKI67
ITGα6
ITGβ1
EGFR
EREG
MT1H
AKR1B10
AKR1C2
KRT1
IVL
FLG
TGM1
CDSN
e
DAPI/K10
DAPI/involucrin
Soft
Glass
f
Cell preconditionning
Clonogenicity on plastic surface
1st generation
2nd
3rd
Glass 72 h
Soft 72 h
O.D. (570nm)
Glass
Soft

◂**Fig. 2** Transcriptomic profiling and colony-forming efficiency. **a** Hierarchical clustering of 200 most differentially expressed genes in keratinocytes cultured for 72 h on soft PAH (S_soft) or glass (S_glass). Green color corresponds to and red color to overexpressed genes. **b** Smear plot of RNA-seq data showing average log signal intensity (x axis) vs. log2 fold change in gene expression (soft PAH/glass). Differentially expressed genes (FDR $q \leq 0.05$) are shown in red for upregulated genes ($n = 808$), in green for downregulated genes (n = 584), and non-significant changes are shown in black. **c** Gene ontology enrichment analysis of the top five molecular functions (GOrilla). Significance of term enrichment by FDR q values is represented by log10 bar values. **d** qPCR validation of 2 unmodulated (black) and 13 modulated (green and red) genes on soft substrate. ($n = 3$) Data are presented as mean ± SD. **e** Human primary keratinocytes were cultured on glass and soft PAH. After 72 h, cells were immunostained for cytokeratin 10 or involucrin (red) and nuclei were counterstained with DAPI (blue). Scale bar: 100 µm. **f** Preconditioned cells grown for 72 h on soft PAH (black) or glass coverslips (gray) were replated on 6-well plates to evaluate colony-forming efficiency for three generations. ($n = 3$) Data are presented as mean ± SD, *P < 0.05, **$P < 0.01$, unpaired T test

during the isolation and amplification process on plastic (> GPa), the keratinocyte appears in a "quiescence-like" state, suggesting a very quick change of keratinocyte phenotype in response to the low compliance (below 15 kPa).

To investigate the particular "quiescience-like" state observed in response to the low compliance, the keratinocytes were cultured on soft PAH and on glass coverslip for 3 days and a phenotype-specific transcriptional profiling was undertaken by RNA-seq analysis (Fig. 2a–c). Consistent with a specific effect of the substrate, the heat map of 200 most differentially expressed genes showed a clustering of the samples by culture conditions over interindividual variability of the three donors (Fig. 2a). A total of 1392 genes were differentially expressed (FDR q value ≤ 0.05) between soft PAH and glass coverslip (Fig. 2b). Among these, 808 genes were expressed at significantly higher levels in soft PAH (gene list available in Online Resource 1), whereas 584 were expressed at significantly lower levels (gene list available in Online Resource 2) compared to glass coverslip. GO pathway analysis of these differentially expressed genes in soft PAH condition revealed an increase in the expression of genes involved in structural constituent of epidermis (23 genes belong to the epidermal differentiation complex located at 1q21 locus), metabolism and anti-oxidative machinery. In parallel, genes that decreased in expression level were preponderantly associated with extracellular matrix binding receptors and cytoskeleton (Fig. 2c). Using real-time RT-PCR on keratinocytes from three other donors, the level of expression of several hits observed in the various GO categories evoked was consistent with RNA-seq data, strengthening the results (Fig. 2d). The transcriptomic profile of the cells cultured on a soft substrate was therefore similar to differentiated keratinocytes. This observation was enhanced at the protein level, since the cells grown on the Soft PAH were all positive for the cytokeratin 10 marker and few cells started to express the involucrin late differentiation marker, while no staining was observed on glass coverslips (Fig. 2e). However, cell cycle-related gene expression levels (*CDKN1A* and *CDKNA2*) were also analyzed and a slight increase in expression level was observed for both genes (Fig. 2d). Hence, the lack of downregulation of genes linked to the cell cycle tended to show that these cells had not fully entered a terminal differentiation pathway and neither could they be related to a quiescent state. Then, preconditioned cells cultured for 3 days on soft PAH or on a glass coverslip were transplanted in 6-well plastic plates (> GPa) to observe colony-forming efficiency over three generations (Fig. 2f). The results showed that the cells previously engaged in the differentiation pathway on soft PAH were able to proliferate again once put back on a rigid substrate. During the two first generations, cells transplanted from soft PAH showed a slight but significant decrease of colony formation compared to cells transplanted from glass. This observation was reversed during the third generation showing that cells from the soft PAH kept an important proliferative potential. However, in both experimental conditions, an overall decrease in proliferative capacity was observed over successive generations.

Finally, since the keratinocyte proliferates normally above 4 kPa, we investigated whether intermediate rigidities could affect the keratinocyte differentiation program. To address this, the keratinocytes were seeded on the surface of medium, rigid PAH and glass coverslips at high density and differentiation was induced by cell confluence and growth factor deprivation at low-calcium concentration. The gene expression level for the proliferation marker *MKI67* was quickly repressed in medium PAH condition as the cells reached confluence, while it was sustained until growth factor depletion in rigid PAH and glass coverslip conditions (Fig. 3a). Regarding the early differentiation marker *KRT10*, its expression increased with time (post-confluence) in a substrate stiffness-dependent manner, reaching a strong expression level on glass coverslip, an intermediary expression on rigid PAH, and no expression on the medium PAH at day 5 (Fig. 3b). Considering the late differentiation markers, *IVL* and *CDSN* expression levels were prematurely increased in medium PAH condition compared to the two other groups (Fig. 3c, d). At day 5, cells cultured on the two PAH displayed a similar higher expression level of the late differentiation markers (*IVL* and *CDSN)* compared to the glass coverslip condition (Fig. 3c, d). These results therefore indicate an adaptive response of the human keratinocytes with respect to rigidity through their capacity to differentiate, the rigidity favoring the expression of early markers of differentiation to the detriment of later markers in contrast to low rigidity.

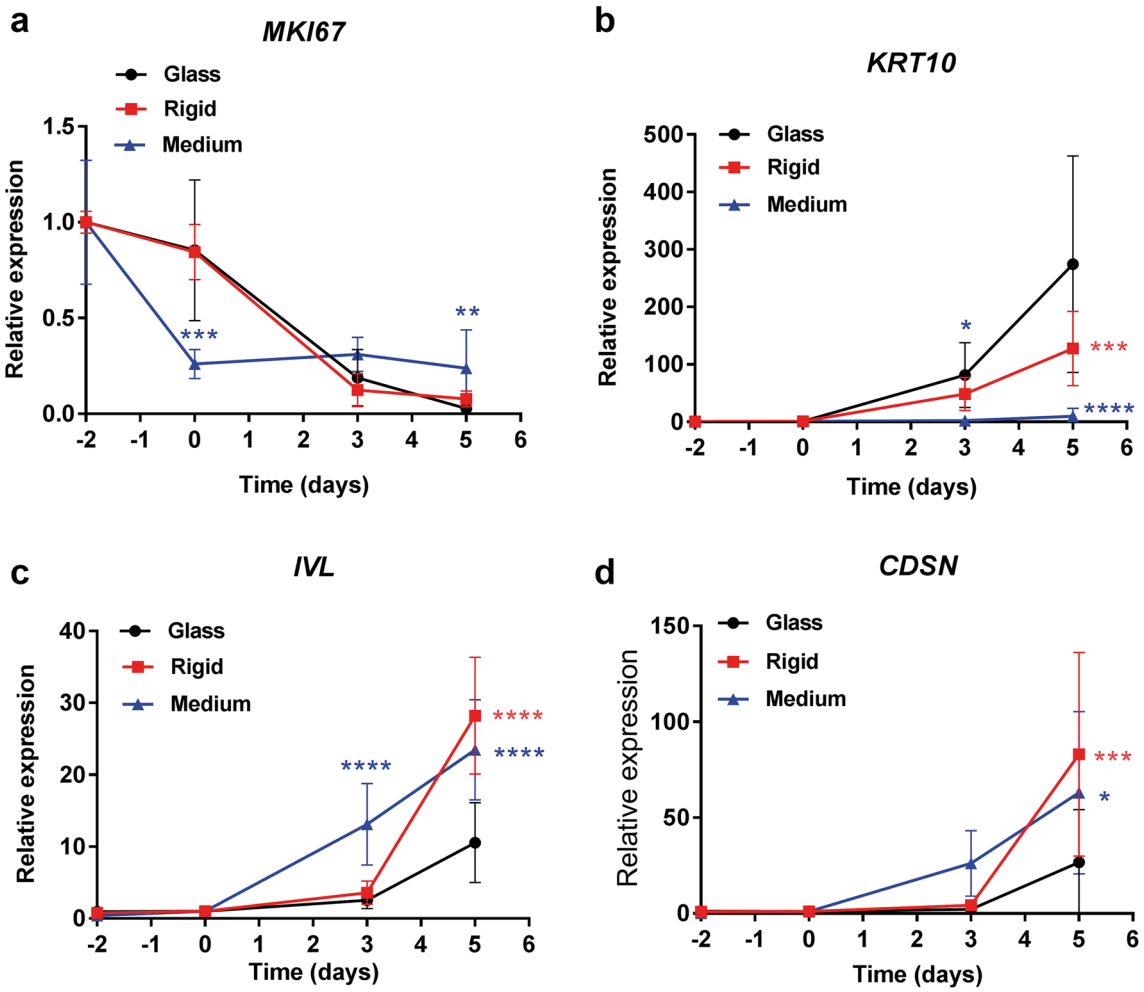

Fig. 3 Substrate stiffness impact on keratinocyte's differentiation. **a**–**d** Cells were plated on medium (blue triangle), rigid (red square) PAH and glass (black dot). mRNA expression was analyzed by qPCR at indicated time (day 0 corresponds to the moment cells reach confluence): proliferation marker *MKI67* (**a**), keratinocyte early differentiation marker *KRT10* (**b**) and keratinocyte late differentiation markers *IVL* (**c**) and *CDSN* (**d**) at the indicated points. ($n=3$) All data are presented as mean ± SD, $^{*}P<0.05$, $^{**}P<0.01$, $^{***}P<0.001$ and $^{****}P<0.0001$, using two-way ANOVA with a Bonferroni post-test, compared to glass condition

Discussion

In the present study, PAH of different rigidities were used to better understand primary human keratinocyte responses in situations where their biomechanical environment is modified. We have shown that soft (~4 kPa) PAH induced terminal differentiation, while rigid PAH (~45 kPa) favored a proliferative state similar to what is observed on glass coverslip or classical plastic culture dishes (> GPa). In addition, we demonstrated that keratinocytes committed in terminal differentiation on the softest environment could reactivate a proliferative response under a more rigid environment suggesting a strong conditioning of the genome by mechanical cell environment. Previous studies demonstrated that the adaptation of keratinocytes to the rigidity of their substrate relies mainly on the possibility for the cells to form focal adhesion points with the underlying ECM [12]. The number and the density of the focal points of adhesion decrease on soft substrates, but the occupation of the surface integrins is essential to prevent the entry into differentiation of the keratinocytes which results from the absence of activation of the signaling cascade focal adhesion kinase (FAK)/extracellular signal-related kinase (ERK)/mitogen-activated protein kinase (MAPK) [22, 26]. Stiffness also promotes proliferation through a synergistic interaction between FAK pathway and EGF receptor signaling [13]. Our observations trend in the same way showing a decrease of focal adhesion points accompanied by a stop of proliferation on the softest substrates (~4 kPa). However, we also emphasize the existence of a stiffness value (< 14 kPa) above which cells equally proliferate, suggesting a nonlinear response of keratinocyte proliferation rate to stiffness. Our results also showed that

the distribution of the focal adhesion points does not vary substantially above this proliferative stiffness value, reinforcing the interrelation between the focal adhesion point assemblies and the capacity for the cell to proliferate. Below the stiffness value allowing proliferation, the keratinocytes undergo an atypical very quick differentiation in response to the low compliance.

The impact of the substrate rigidity is much more progressive with respect to the differentiation capacity of the keratinocytes. Trappmann et al. reported a similar correlation between PAH stiffness increase and involucrin synthesis inhibition in keratinocytes at 24 h post-seeding [22]. Using monolayer keratinocyte cultures, we showed that the lesser the stiffness, the more the keratinocytes are able to express markers of late differentiation such as involucrin and corneodesmosin. In contrast, the early differentiation marker, cytokeratin 10, increases with increasing rigidity. Moving towards the critical proliferative stiffness value, *KRT10* gene expression is not observed at all after 3 days. However, this does not exclude the fact that this marker can be expressed at an earlier time, as evidenced by the presence of cytokeratin 10 in the softest hydrogels 3 days. Our results support the idea that on softer substrates, keratinocytes are quickly committed to terminal differentiation. Consistent with these observations, the mechanical measurements made on the human skin at different ages showed a reduced elastic modulus of 10 kPa at 30, 7.5 kPa at 60 years and 5.3 kPa at 80 year old [30]. Hence, changes in the dermis stiffness with aging could explain the phenotypic disturbances observed in keratinocytes leading to an alteration of epidermal homeostasis, and particularly the epidermal thinning [17].

The modulation of the differentiation being gradual according to rigidity, it cannot be directly related to the density of the focal adhesion points that were constant above the proliferative stiffness value. Indeed, differentiating keratinocytes are supposed to leave the basal membrane and no longer establish focal adhesion points. Our results showed that the cytoskeleton organization changes in a more gradual way with rigidity through the clustering of actin filaments in the peri-cytoplasmic region, beneath the plasma membrane, and across the cytoplasm. Interestingly, the spectrin cytoskeleton, a crosslinker of actin filaments and mainly implicated in cell shape maintenance [16], is abundant in differentiated keratinocytes, and the disorganization of this architecture prevents the correct differentiation of the keratinocyte [31]. Moreover, recent studies have shown that the spectrin cytoskeleton plays an important role in the mechanotransduction of osteocytes [28], so it would be interesting to explore the involvement of the stiffness related to spectrin cytoskeleton changes on keratinocyte differentiation.

Thus, there would be an optimal rigidity allowing to maintain a proliferative state of keratinocytes and their complete differentiation capacity as previously demonstrated in mouse skin wound healing using poly(amidoamine) and poly(*n*-isopropyl acrylamide) hydrogels of varying rigidity [4]. Indeed, the authors indicated that hydrogels of medium rigidity (in the order of the kPa) improve wound healing in vivo by promoting fibroblast transformation, wound closure and proliferation of keratinocytes; while very soft (< kPa) or more rigid (~ 50 kPa) hydrogels hinder these processes. Interestingly, our results are concordant with the delay of proliferation but also show a premature expression of late differentiation markers on soft substrates. These observations are consistent with the histological description of an aged epidermis in which the suprabasal layers decrease in number, giving rise to a thinner epidermis, although the aged cells are capable of forming a stratum corneum [17]. Together with our results, this suggests that soft substrate would confer an aged phenotype to cells obtained from young donors as is the case in our study.

We also studied the phenotype reversibility of cultured keratinocyte differentiation on the softest substrates. In the late 80s, Adams and Watt demonstrated that keratinocytes suspended in methylcellulose leave the cell cycle and express terminal differentiation genes such as involucrin after only 24 h [2]. The addition of fibronectin in the suspension abrogated the expression of the differentiation genes but did not allow re-inducing the cell cycle. These previous data suggest that the occupation of surface integrins by their ligand is not sufficient to promote proliferation and that it is necessary for the keratinocyte to supplement this signaling by other means of mechanical perception. In our study, we pushed keratinocyte culture up to 3 days on the softest substrates to commit them more downstream in the differentiation program despite low-calcium concentration and lack of cell–cell junctions. Gene expression profile is strongly modified, probably through epigenetic reprogramming insofar as a majority of the genes contained in the epidermal differentiation complex is expressed [1]. At the protein level, all the cells grown on Soft PAH express the cytokeratin 10 marker, and several cells already produce the involucrin late differentiation marker. Our results demonstrate that the differentiated cells replated on a rigid substrate were able to readapt to this new biomechanical environment and to start proliferating again with a colony-forming efficiency slightly lower during the two first generations than cells that have not been differentiated and even higher during the third generation. This increase during the third generation could be explained by the fact that cells from Soft PAH were less divided during the two first generations, thus preserving their proliferative potential compared to cells preconditioned on glass coverslips. It therefore appears that the keratinocytes initially grown at low density on soft substrates preserved an important proliferative potential despite the prior induction of differentiation. Previously, Poumay and Pittelkow showed that

an entry into differentiation induced by a high concentration of calcium or a depletion in growth factors does not alter the clonogenic capacity of keratinocytes and that a decrease is observed only if the keratinocytes are pushed to confluence [19]. This suggests that keratinocyte clonogenicity or proliferation potential is intimately related to their level of confluence, although the very early markers of cytokeratin 1 and 10 were only studied. However, this hypothesis remains plausible in our case.

In conclusion, we confirmed here the response of primary human keratinocytes to soft substrate by the decrease of their adhesion focal points and proliferation, and we demonstrated a quick commitment of these cells in terminal differentiation. Moreover, this study turns out that the induction of terminal differentiation on a soft substrate is reversible and open the way to interesting models to study the genome plasticity of keratinocytes. Extensive future studies of the reversible aspect of these reprogramming mechanisms would be helpful to discover new targets in pathophysiological situations displaying impaired epidermal differentiation, notably when dermal mechanical properties are modified.

Acknowledgements This work is supported by Isispharma France. Choua Ya is a recipient of a PhD grant from the French National Association of Research and Technology (ANRT). Mariana Carrancá is supported by a PhD grant from the Région Auvergne Rhône Alpes.

Compliance with ethical standards

Conflict of interest The authors have no conflict of interest to disclose.

References

1. Abhishek S, Palamadai Krishnan S (2016) Epidermal differentiation complex: a review on its epigenetic regulation and potential drug targets. Cell J 18:1–6
2. Adams JC, Watt FM (1989) Fibronectin inhibits the terminal differentiation of human keratinocytes. Nature 340:307–309. https://doi.org/10.1038/340307a0
3. Blanpain C, Fuchs E (2009) Epidermal homeostasis: a balancing act of stem cells in the skin. Nat Rev Mol Cell Biol 10:207–217. https://doi.org/10.1038/nrm2636
4. Chen S, Shi J, Xu X, Ding J, Zhong W, Zhang L, Xing M, Zhang L (2016) Study of stiffness effects of poly(amidoamine)-poly(*n*-isopropyl acrylamide) hydrogel on wound healing. Coll Surf B Biointerfaces 140:574–582. https://doi.org/10.1016/j.colsurfb.2015.08.041
5. Eden E, Navon R, Steinfeld I, Lipson D, Yakhini Z (2009) GOrilla: a tool for discovery and visualization of enriched GO terms in ranked gene lists. BMC Bioinform 10:48. https://doi.org/10.1186/1471-2105-10-48
6. Edwards C, Marks R (1995) Evaluation of biomechanical properties of human skin. Clin Dermatol 13:375–380
7. El-Domyati M, Attia S, Saleh F, Brown D, Birk DE, Gasparro F, Ahmad H, Uitto J (2002) Intrinsic aging vs. photoaging: a comparative histopathological, immunohistochemical, and ultrastructural study of skin. Exp Dermatol 11:398–405
8. Evans ND, Oreffo RO, Healy E, Thurner PJ, Man YH (2013) Epithelial mechanobiology, skin wound healing, and the stem cell niche. J Mech Behav Biomed Mater 28:397–409. https://doi.org/10.1016/j.jmbbm.2013.04.023
9. Hinz B, Mastrangelo D, Iselin CE, Chaponnier C, Gabbiani G (2001) Mechanical tension controls granulation tissue contractile activity and myofibroblast differentiation. Am J Pathol 159:1009–1020. https://doi.org/10.1016/S0002-9440(10)61776-2
10. Hsu CK, Lin HH, Harn HI, Hughes MW, Tang MJ, Yang CC (2018) Mechanical forces in skin disorders. J Dermatol Sci 90:232–240. https://doi.org/10.1016/j.jdermsci.2018.03.004
11. Jor JW, Parker MD, Taberner AJ, Nash MP, Nielsen PM (2013) Computational and experimental characterization of skin mechanics: identifying current challenges and future directions. Wiley Interdiscip Rev Syst Biol Med 5:539–556. https://doi.org/10.1002/wsbm.1228
12. Kenny FN, Connelly JT (2015) Integrin-mediated adhesion and mechano-sensing in cutaneous wound healing. Cell Tissue Res 360:571–582. https://doi.org/10.1007/s00441-014-2064-9
13. Kenny FN, Drymoussi Z, Delaine-Smith R, Kao AP, Laly AC, Knight MM, Philpott MP, Connelly JT (2018) Tissue stiffening promotes keratinocyte proliferation through activation of epidermal growth factor signaling. J Cell Sci 131:jcs215780. https://doi.org/10.1242/jcs.215780
14. Law CW, Chen Y, Shi W, Smyth GK (2014) voom: precision weights unlock linear model analysis tools for RNA-seq read counts. Genome Biol 15:R29. https://doi.org/10.1186/gb-2014-15-2-r29
15. Liao Y, Smyth GK, Shi W (2013) The Subread aligner: fast, accurate and scalable read mapping by seed-and-vote. Nucleic Acids Res 41:e108. https://doi.org/10.1093/nar/gkt214
16. Liem RK (2016) Cytoskeletal Integrators: the spectrin superfamily. Cold Spring Harb Perspect Biol 8:a018259. https://doi.org/10.1101/cshperspect.a018259
17. Mainzer C, Remoue N, Molinari J, Rousselle P, Barricchello C, Lago JC, Sommer P, Sigaudo-Roussel D, Debret R (2018) In vitro epidermis model mimicking IGF-1-specific age-related decline. Exp Dermatol 27:537–543. https://doi.org/10.1111/exd.13547
18. McCarthy DJ, Chen Y, Smyth GK (2012) Differential expression analysis of multifactor RNA-Seq experiments with respect to biological variation. Nucleic Acids Res 40:4288–4297. https://doi.org/10.1093/nar/gks042
19. Poumay Y, Pittelkow MR (1995) Cell density and culture factors regulate keratinocyte commitment to differentiation and expression of suprabasal K1/K10 keratins. J Invest Dermatol 104:271–276
20. Ritchie ME, Phipson B, Wu D, Hu Y, Law CW, Shi W, Smyth GK (2015) limma powers differential expression analyses for RNA-sequencing and microarray studies. Nucleic Acids Res 43:e47. https://doi.org/10.1093/nar/gkv007
21. Robinson MD, McCarthy DJ, Smyth GK (2010) edgeR: a Bioconductor package for differential expression analysis of digital gene expression data. Bioinformatics 26:139–140. https://doi.org/10.1093/bioinformatics/btp616
22. Trappmann B, Gautrot JE, Connelly JT, Strange DG, Li Y, Oyen ML, Cohen Stuart MA, Boehm H, Li B, Vogel V, Spatz JP, Watt FM, Huck WT (2012) Extracellular-matrix tethering regulates stem-cell fate. Nat Mater 11:642–649. https://doi.org/10.1038/nmat3339
23. Varani J, Dame MK, Rittie L, Fligiel SE, Kang S, Fisher GJ, Voorhees JJ (2006) Decreased collagen production in chronologically aged skin: roles of age-dependent alteration in fibroblast function and defective mechanical stimulation. Am J Pathol 168:1861–1868. https://doi.org/10.2353/ajpath.2006.051302
24. Waldera Lupa DM, Kalfalah F, Safferling K, Boukamp P, Poschmann G, Volpi E, Gotz-Rosch C, Bernerd F, Haag L,

Huebenthal U, Fritsche E, Boege F, Grabe N, Tigges J, Stuhler K, Krutmann J (2015) Characterization of skin aging-associated secreted proteins (SAASP) produced by dermal fibroblasts isolated from intrinsically aged human skin. J Invest Dermatol 135:1954–1968. https://doi.org/10.1038/jid.2015.120

25. Wang Y, Wang G, Luo X, Qiu J, Tang C (2012) Substrate stiffness regulates the proliferation, migration, and differentiation of epidermal cells. Burns 38:414–420. https://doi.org/10.1016/j.burns.2011.09.002
26. Watt FM, Kubler MD, Hotchin NA, Nicholson LJ, Adams JC (1993) Regulation of keratinocyte terminal differentiation by integrin-extracellular matrix interactions. J Cell Sci 106(Pt 1):175–182
27. Wong VW, Akaishi S, Longaker MT, Gurtner GC (2011) Pushing back: wound mechanotransduction in repair and regeneration. J Invest Dermatol 131:2186–2196. https://doi.org/10.1038/jid.2011.212
28. Wu XT, Sun LW, Yang X, Ding D, Han D, Fan YB (2017) The potential role of spectrin network in the mechanotransduction of MLO-Y4 osteocytes. Sci Rep 7:40940. https://doi.org/10.1038/srep40940
29. You H, Padmashali RM, Ranganathan A, Lei P, Girnius N, Davis RJ, Andreadis ST (2013) JNK regulates compliance-induced adherens junctions formation in epithelial cells and tissues. J Cell Sci 126:2718–2729. https://doi.org/10.1242/jcs.122903
30. Zahouani H, Pailler-Mattei C, Sohm B, Vargiolu R, Cenizo V, Debret R (2009) Characterization of the mechanical properties of a dermal equivalent compared with human skin in vivo by indentation and static friction tests. Skin Res Technol 15:68–76. https://doi.org/10.1111/j.1600-0846.2008.00329.x
31. Zhao KN, Masci PP, Lavin MF (2011) Disruption of spectrin-like cytoskeleton in differentiating keratinocytes by PKCdelta activation is associated with phosphorylated adducin. PLoS One 6:e28267. https://doi.org/10.1371/journal.pone.0028267